Graphical Abstract

Click here to access/download;Graphical Abstract (for review);vf GA.pdf

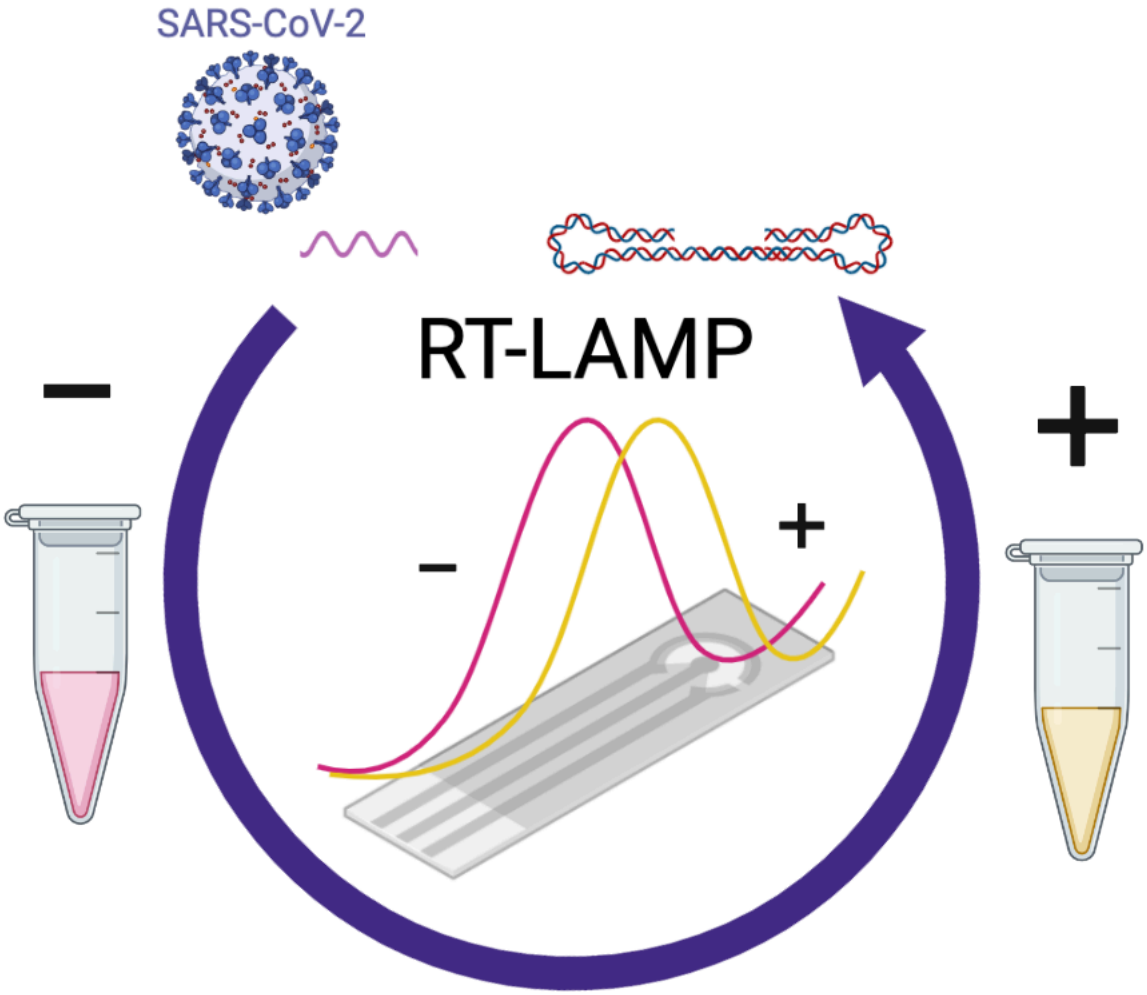

Highly sensitive electrochemical detection for loop-mediated isothermal amplification (RT-LAMP-ED) of SARS-CoV-2 using phenol red as dual indicator

P. Rioboó-Legaspi[1], A. González-López[1], J.F. Beltrán-Sánchez[2], M.D. Cima-Cabal[3]*, M.M. García-Suárez[3], A.J. García Sánchez[2], T. Fernández-Otero[2], J. García Haro[2], E. Costa-Rama[1], M.T. Fernández-Abedul[1]*

[1]*Departamento de Química Física y Analítica, Facultad de Química, Universidad de Oviedo, Spain.*

[2]*Departamento de Tecnologías de la Información y las Comunicaciones, Universidad Politécnica de Cartagena, Murcia, Spain.*

[3]*Escuela Superior de Ingeniería y Tecnología, Universidad Internacional de La Rioja, Spain*

**Corresponding authors: M.T. Fernández-Abedul, email: mtfernandeza@uniovi.es; M. D. Cima-Cabal, email: dolores.cima@unir.net.*

ABSTRACT

The current COVID-19 pandemic has made patent the need for rapid and cost-effective diagnostic tests, crucial for future infectious outbreaks. qPCR is still considered the gold standard for pathogen detection, but relies on centralized, expensive equipment, leading to major difficulties for on-site detection. To overcome these limitations, loop-mediated isothermal amplification (LAMP), arises as a promising alternative. However, the development of simple, affordable, sensitive, and robust methodologies is still key for achieving quantitative point-of-care analysis.

In this work we have developed a sensitive, fast, and simple SARS-CoV-2 detection methodology combining reverse-transcription LAMP with electrochemical detection. This is based on the oxidation of phenol red (PR), a visual LAMP indicator that is also electroactive. Thus, we have developed a quantification method with a limit of detection of 21copies per reaction. This methodology has been applied to the analysis of nasopharyngeal swab samples, resulting in total concordance with clinical

RT-qPCR results. We have also designed and fabricated a small portable heater for LAMP purposes in extra-laboratory facilities, with a performance comparable to a commercial thermal cycler.

KEYWORDS

Low-cost analysis; electrochemical detection; screen-printed electrodes; phenol red; isothermal amplification (LAMP); SARS-CoV-2

INTRODUCTION

The COVID-19 pandemic, caused by SARS-CoV-2, has highlighted the need for point-of-care (POC) diagnostics, providing rapid, accurate and on-site results, so the infected individual can be quickly isolated [1], with analytical devices delivered to end users. Although several vaccines have been developed and successfully administered [2], the rise of new variants and the refusal or delay in vaccination makes essential the development of decentralized, yet sensitive tests [3]. Aside from COVID-19 pandemic, attention to other zoonotic outbreaks is required, with field-deployable diagnostics technology ready.

The gold-standard for SARS-CoV-2 testing is RT-qPCR (reverse-transcription quantitative polymerase chain reaction) which relays on amplification and detection of the viral genome [4] with exceptional sensitivity and specificity, but requiring pre-processing steps, expensive equipment, and trained personnel. Other option is the use of POC tests, such as antigen or antibody assays [5] that can be even performed by the end user but provide frequently lower sensitivity and high false negative rate, especially in asymptomatic patients [6].The optimal middle ground would be a diagnostic tool providing sensitivity and specificity as close as possible to RT-qPCR, but also portable, fast, easy-to-use and with affordable costs.

An approachable alternative is RT-LAMP (reverse-transcription loop-mediated isothermal amplification), performed at *ca.* 65 ºC throughout the whole reaction process, with no need of temperature cycles, and with shorter reaction time. It relies on the formation of loop-shaped secondary structures along the amplification [7]. Furthermore, this technique presents a sensitivity comparable to RT-qPCR in detecting COVID-19 in the acute phase of the illness, being an appropriate alternative diagnostic tool [8].

Conventional LAMP reaction readouts rely on turbidimetric, colorimetric and fluorimetric approaches. Observing changes by the naked eye is simple and useful for semiquantitative purposes. However,

quantitative analysis requires the implementation of instrumental methodologies, with additional workflow steps that difficult the decentralization. For this purpose, electrochemical techniques have provided sensitive methods yet robust and decentralizable. Several approaches have been implemented to detect and/or quantify LAMP products, all of them relying on intrinsic changes that occur in the reaction solution (e.g., DNA synthesis, pH drop or inorganic pyrophosphate release). Some direct strategies have been proposed, as those based on the change of conductivity and resistance [9] or pH, employing e.g., a hydrogen ion selective electrode containing a ionophore membrane [10] or a combined iridium oxide/carbon paste two-electrode system [11]. Alternatively, electrodes modified either with conductive polymers or metal nanoclusters which formal potential changes with pH [12] have been also employed. Indirect strategies are based on the use of electrochemical reporter molecules that can be either free in the reaction medium, such as Hoechst-33258 [13] or conjugated to DNA-probes as in the case of ferrocene-labelled strands [14].

Creative strategies are very interesting but the introduction of more reagents and steps increases costs and complicates the procedure. However, approaches based on a change in the electrochemical process of molecules are already present in commercial LAMP kits, usually as colorimetric indicators, do not suppose an important workflow change and can provide extra information. On the other hand, as the redox species is always at high concentration, a clear, precise, and well-defined analytical signal could be monitored. For this purpose, phenol red (PR) visual indicator is an excellent option since it is a widely used colorimetric probe for LAMP detection, coming already pre-mixed in many commercial kits. It presents a characteristic oxidation process that shifts to more positive potentials as pH drops, which can be very useful for electrochemical detection in slightly buffered media as is the case of LAMP reactions [15].

In this work we have developed a fast, sensitive, and precise SARS-CoV-2 electrochemical detection for RT-LAMP reactions (RT-LAMP-ED). This methodology, with diagnostic potential, can be easily performed with simple portable devices. For that purpose, we have developed a small lightweight

heater that can perform isothermal LAMP amplifications outside the laboratory or healthcare facilities. This is the first time that PR is used not only as colorimetric but also as electrochemical indicator for the determination of SARS-CoV-2 in clinical nasopharyngeal samples.

MATERIALS AND METHODS

Sample collection. Nasopharyngeal (NP) swab samples were collected at the Central University Hospital of Asturias (HUCA). Swabs were introduced in a microcentrifuge tube containing 500 µL of 10 mM Tris-EDTA (TE) pH 8.0 buffer. Samples were inactivated at 95 ºC for 5 min prior to its transportation [16] to our laboratory. The effect of proteinase K (Recombinant, PCR-Grade, ThermoFisher) treatment of samples was assessed at a final concentration of 0.04 mg·mL^{-1}. This study was carried out in accordance with the recommendations of the Ethical Committee on Regional Clinical Research of the Principality of Asturias.

LAMP Assay. Three sets of six specific LAMP primers were used based on sequences from previous studies [17–19] to amplify fragments N, N1 and S of SARS-CoV-2 genome. Primer sequences can be found in Table S1.

The reaction mix using WarmStart® Colorimetric LAMP 2X Master Mix (DNA & RNA) (New England Biolabs) contained 1x master mix (including *Bst* 2.0 DNA Polymerase and phenol red), 0.7 mM dUTG, primer mix (1.6 µM each FIP and BIP primer, 0.2 µM each F3 and B3 primer and 0.4 µM each LoopF and LoopB primer), 0.3 U Antarctic Thermolabile UDG (Uracyl-DNA-Glycosylase) (New England Biolabs) and PCR-grade dH_2O (Invitrogen UltraPure™ Distilled Water (DNase/RNAse free), Life Technologies) up to 24 µL of final volume. 1 µL of template SARS-CoV-2 RNA (VR-1986D, ATCC®), if required, was added at the desired concentration. All concentrations are indicated as copies·µL^{-1} of standard or sample solution. 1 µL of PCR-grade dH_2O was added to negative (non-template) control reactions. All reactions were performed on low-retention, nuclease-free PCR grade tubes (PCR-02-L-C, Axygen™) under sterile conditions in a laminar flow hood. To prevent carryover contaminations,

all the equipment was cleaned with 5% sodium-hypochlorite solution. Reactions were incubated in a thermal cycler (Veriti 96 Well Thermal Cycler, Applied Biosystems) at 65 ºC for 30 min, with an initail step of 10 min at 37 ºC for UDG activity. If using the portable heater (with constant 65 ºC) this UDG step was carried out at room temperature prior to amplification. Samples were then kept at 4 ºC for improved colour contrast.

Electrochemical detection. Electrochemical measurements of the amplifications were performed using thick-film electrodes (S1PE, Micrux Technologies) connected to a µAUTOLAB TYPE III potentiostat (Metrohm), which was controlled by NOVA Software 2.1.5, through a box connector (ED-SPE-BOX, Micrux Technologies). The screen-printed electrodes (SPEs, dimensions 27.5x10.1x0.35 mm) consist of three electrodes: a circle-shaped working electrode with a 3-mm diameter and a counter electrode, both made of carbon ink, and a reference electrode made of silver ink. To perform the electrochemical measurements, 25 µL were deposited covering the three electrodes. The measurements were recorded at room temperature and one three-electrode card was used for each measurement. Cyclic voltammograms (CVs) were recorded scanning the potential from +0.2 to +0.9 V at a scan rate of 0.1 $V \cdot s^{-1}$.

Image Analysis. Images from the calibration curve were analysed using the open-source image processing software ImageJ [20]. Green (from RGB) and hue (from HSV) channel intensity values were measured for quantification. For green channel analysis, images were RGB split and then measured in the green channel, as it has been previously reported [21]. For hue analysis, hue was rotated 140º using the HueRotation plugin. Then a HSB split was performed, and a subsequent hue quantification was carried out [22].

Statistics. Results in this study are represented as mean value ± standard deviation (SD). Differences between data groups were analysed using Student's T-test (two-tailed, non-paired samples). Samples were previously tested for normality and homogeneity of variance using the Shapiro-Wilk and

Bartlett's test, respectively. Differences were considered statistically relevant at $p<0.05$ (*), $p<0.01$(**) and $p<0.005$ (***).

Small portable heater for LAMP amplifications

The small and portable heater for LAMP purposes is comprised of a heater cavity with room for a set of samples (approximately 6 to 8 PCR tubes) and a 3D printed PLA case and lid. This cavity is heated by an internal heating surface, which is electronically controlled by a PWM (pulse width modulation) signal to keep the temperature fine-tuned during the amplification process.

The heating system is composed by a resistive film (DuPont™ Kapton® RS) powered by a boost converter, which converts the voltage of a battery or wall adapter to the voltage required by the heater. To control and tune the voltage value provided by the converter, a PWM signal switches the power supplied to the heating film. The temperature is measured by a thermocouple sensor located in the heating surface. The acquired temperature signal is dispatched to the microcontroller, which, by comparison with the target temperature value and a PID control loop, establishes the pulse width of the PWM signal. This signal sets the voltage switching process. To achieve the portability feature, the power can be supplied from a wall adapter, but also from a portable power bank. The heating temperature and working time re programmable. The device presents a LED light indicating whether it is heating up (green light) or has already reached a stable temperature (blue light). The temperature of the heater was assessed using a digital thermometer with a temperature probe (UT320, UNI-T).

RESULTS

Electrochemical detection of the N gene amplification

A fragment of the nucleocapsid gene (N gene) of the SARS-CoV-2 sequence was first amplified to assess the possibility of performing a quantitative electrochemical detection. For this purpose, RT-

LAMP reactions of the N fragment were performed. The results of this assay can be observed in Figure 1A (top). Three negative (non-template) controls (NC) were assessed, as well as three positive controls (PC, 2148 RNA copies·μL^{-1}). A colour shift from pink to yellow can be observed when the RT-LAMP reaction has occurred. For the electrochemical detection, the CV results obtained show the anodic process of PR, with a clear shift towards more positive potentials from negative to positive controls (Figure 1A, bottom). The precision of the peak potential (E_p) is excellent: 557 ± 5 mV for negative and 602 ± 7 mV for positive controls. This suggests that the difference in E_p could be an adequate analytical signal. However, the difference in the peak current intensity (I_p) is not significant, with a value of 1.52 ± 0.03 µA for negative controls and 1.48 ± 0.02 µA for positive controls.

Based on these results, different readout possibilities for the electrochemical measurements can be established (Figure 1B). The main response parameters to be considered in a CV are E_p and I_p. The first is relevant for qualitative analysis, since each species is oxidized/reduced at a specific potential for a given electrochemical system, phenol red/LAMP medium/SPE in this case. However, as the pH medium changes and protons are involved in the PR redox reaction, a movement in its E_p is produced. Therefore, this parameter (or its shift, ΔE_p) can be employed with quantitative purposes, as is proportional to the concentration of protons. In the LAMP reaction, protons are released when nucleotides are added to the strand and then, a decrease in pH is produced. Since PR moves towards more positive potentials with decreasing pH, this potential shift can be correlated with the number of initial RNA copies and calibrated for different concentrations of viral RNA. On the other hand, I_p can be used for quantitative purposes since it is proportional to the concentration of the electroactive species. In this case, there is not a significant change (ΔI_p) for PR. However, in the CV curves of Figure 1B, a difference in the current intensity measured at a fixed potential corresponding to the peak potential of the negative control or lower (E_p, $E_{p/1.33}$, $E_{p/2}$…), can also be measured (ΔI_E). As positive reactions experiment a shift towards higher potential values, they will have lower intensity current at the given potential when compared with negative controls. Then, it could be also calibrated for different concentrations of viral RNA.

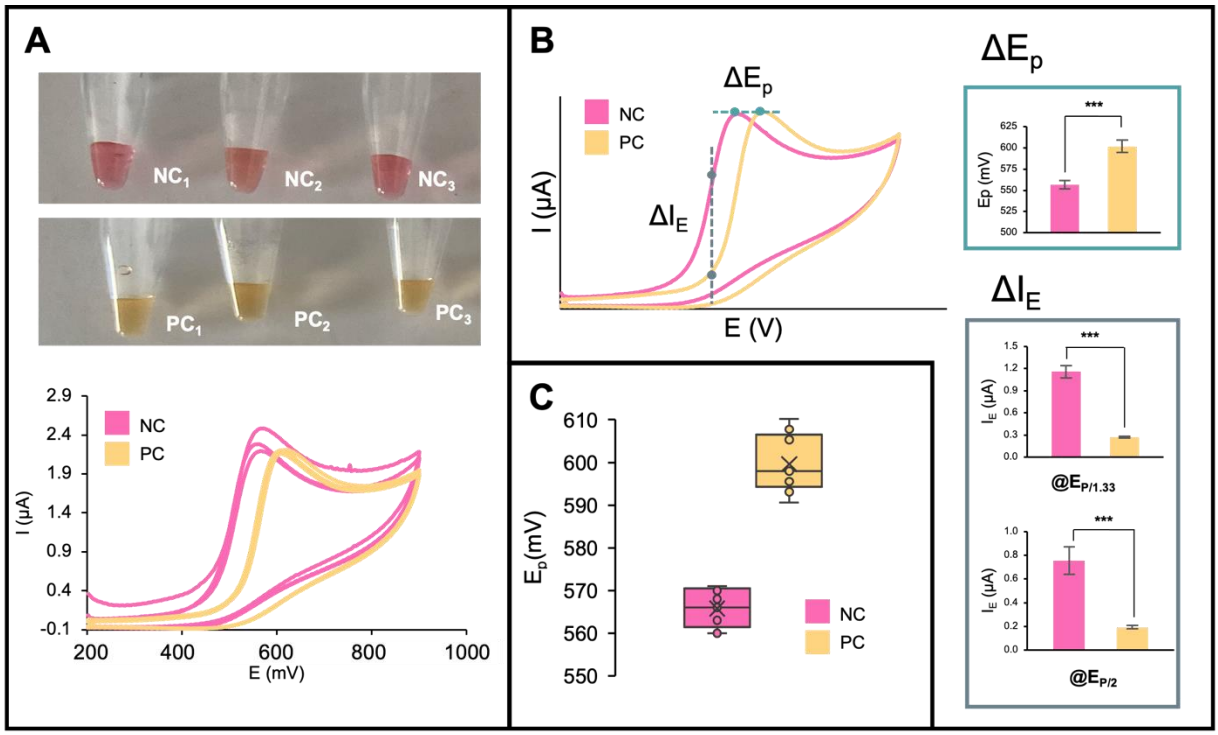

Figure 1. Electrochemical detection of the LAMP amplification of the N fragment of SARS-CoV-2. A: Visual (top) and electrochemical (bottom) result of the amplification. B: Different electrochemical readout possibilities. Analytical signals obtained. ***:p<0.005. Error bars represent the SD for three different amplifications. C: Box-and-whiskers plot for 10 negative reactions (pink) and 10 positive reactions (yellow). NC: negative control; PC: positive control (2148 RNA copies·µL^{-1}).

Figure 1B shows the two possible analytical signals obtained from CVs recorded after RT-LAMP reactions. Regarding ΔE_p, we can observe a significant increase for positive samples. When considering ΔI_E, we can observe a significant decrease at a potential where the peak intensity is either 75% or 50% (half-peak potential) of the NC peak current intensity ($@E_{p/1.33}$ and $@E_{p/2}$, respectively). This gives two valuable interpretations of the CVs to choose the best analytical signal.

The robustness of this method was evaluated measuring 20 amplifications (10 NCs and 10 PCs, with 2148 copies·µL^{-1}) of the same fragment using 20 different SPEs (Figure S1). Figure 1C shows the box-and-whiskers plot obtained representing ΔE_p for both groups. The relative standard deviation was 1.2% for positive and 0.8% for negative amplifications, indicating a high precision of the LAMP-ED

methodology. The fact that PR is present at high concentration and shows a clearly defined signal is probably the main reason.

Calibration curve for SARS-CoV-2 quantification using RT-LAMP-ED

Besides N fragment, other target sequences were evaluated to optimize the detection methodology. Two additional different fragments were amplified, comprising a sequence belonging to the S (spike protein) gene and the N1 fragment of the nucleocapsid gene (amplification results and fragment locations within SARs-CoV-2 genome can be seen in Figure S2). Starting from 3 different initial concentrations of RNA, the ΔE_p after LAMP amplification was measured. As it can be observed in Figure S3, 107 and 214 copies·μL^{-1} can be clearly differentiated from NC only in the case of the N1 fragment. A linear relationship can also be observed when amplifying this region with a change of *ca.* 16 mV per order of magnitude of RNA concentration. In the case of S and N sequences, the values for 107 and 214 copies were below the dashed lines, that correspond to 3 times the SD of the NC signal. Therefore, the fragment N1 was considered for further studies.

To develop a quantitative detection method, a calibration curve with different initial concentrations of RNA was performed, amplifying the N1 region (Figure 2A). RT-LAMP reactions were performed thrice, and an initial visual (naked eye) assessment was performed (Table at Figure 2A). Although amplifications starting from 107 copies·μL^{-1} can be clearly distinguished as positive, it is difficult to discern those with lower copy number.

Calibration curves based on electrochemical measurements (Figures 2C and 2D) were obtained measuring both ΔE_p and ΔI_E at a potential corresponding to a 75% and 50% intensity of that of the peak potential for NCs ($E_{p/1.33}$ and $E_{p/2}$, i.e., 556 and 534 mV respectively). The ΔE_p (compared with NCs) shows a good linearity with the starting RNA concentration over almost three orders of magnitude. Figure 2D presents values of $\Delta I@E_{p/1.33}$ when compared to NCs, while Figure S4 shows the values of $\Delta I@E_{p/2}$, with a lower coefficient of determination. Then, ΔE_p was chosen for further

studies, as it shows good linear fit and sensitivity and it simplifies data analysis. The potential shifts 16.2 mV per order of magnitude, which agrees with this commented for Figure S3, indicating the robustness of the LAMP-ED methodology.

Reactions were also analysed using ImageJ. Pictures after amplification were captured and analysed using ImageJ following two procedures reported in the bibliography [21,22] for PR based LAMP amplifications. The comparison of both analyses (Figure S5) shows that hue values, albeit showing lower increases, follow a linear tendence. Green values appear to be very sensitive to irregular brightness, as this method was first proposed for paper-based amplification, where image artifacts were not as relevant. On the other hand, the method proposed by Scott et al. relies on tube-based amplifications, where uneven brightness can be a common artifact, and thus this method is more suitable for our analysis. Green channel intensity is an easier parameter to obtain in terms of image processing, and brightness and reflections can be avoided using specialized image acquisition equipment [23]. The curve using hue values is shown in Figure 2A (right).

An amplification starting from 5 copies per reaction was also performed (grey dataset in Figures 2B, 2C, 2D and S4) but was not considered in the equation of the calibration curve as it was under our threshold value (3 times the standard deviation of the NC value) or showed a high variance. In any case, it fitted the linear trend of the ΔE_p calibration curve ($R^2 = 0.992$) as well as the current decrease curve ($R^2 = 0.991$). The increase in variance of LAMP results when starting from low copy number (from 1 to 100 copies per reaction) has been previously reported compared to qPCR [4]. If dealing with low copy number samples, multiple amplifications should be thus performed to prevent false negative results. The RT-LAMP-ED method would then provide a qualitative (positive/negative) response, but if quantification is desired, a dilution of the sample should be done.

The limit of detection (LOD) calculated as 3 times the SD of the negative control divided by the slope of the linear fit is 1 copy·μL^{-1}. However, we have stablished a more practical LOD considering a cut-off signal value of 11.5 mV, based on the lowest discernible concentration (21 copies·μL^{-1}). Any

electrochemical measurement with a value below this would be considered a negative amplification. Based on the same approach, considering the higher concentration of the linear dynamic range (1428 copies·µL^{-1}) any electrochemical measure over 42.4 mV would be positive with a concentration of RNA over 1428 copies·µL^{-1}. Samples with an electrochemical signal between 11.5 and 42.4 mV could be precisely quantified.

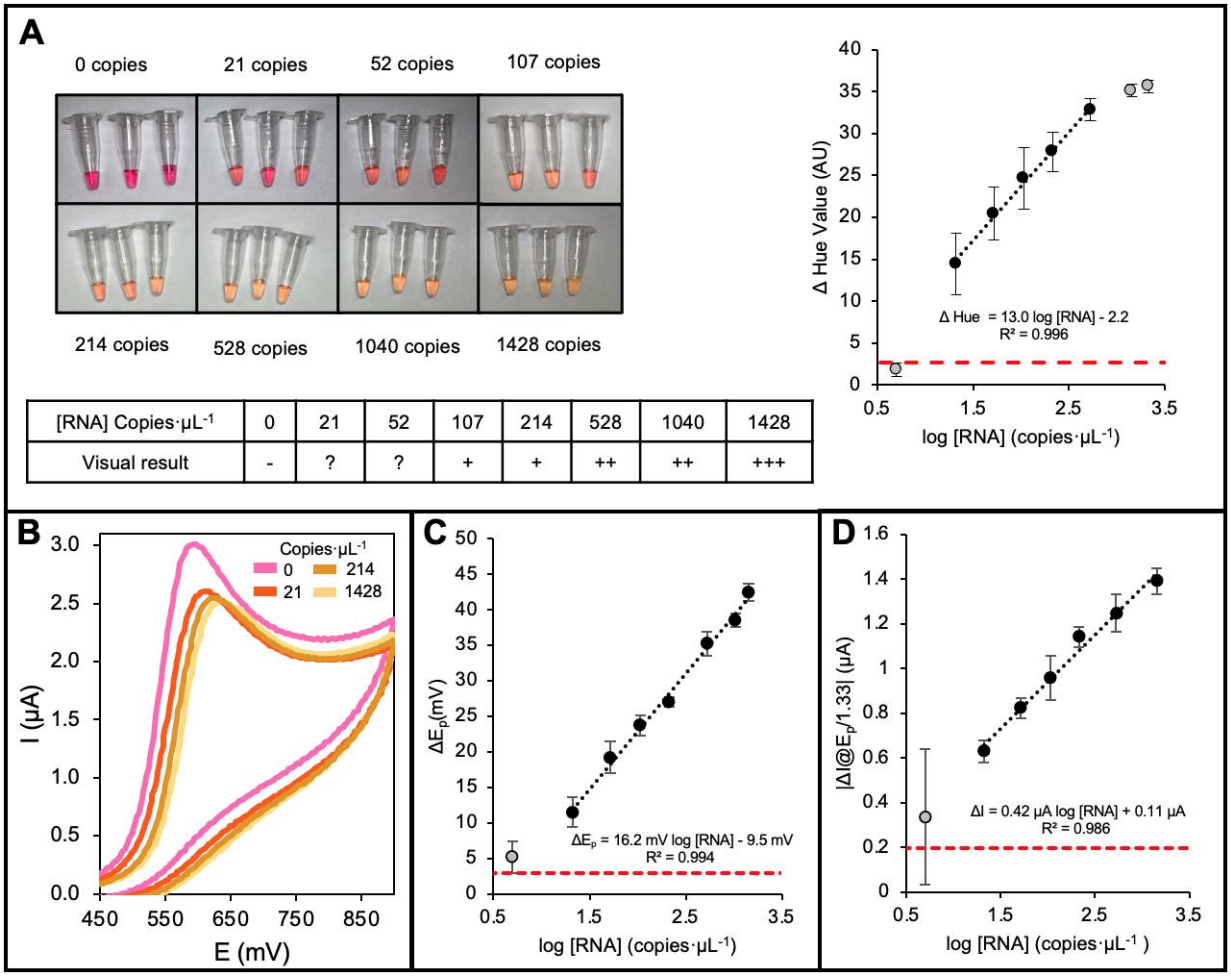

[RNA] Copies·µL^{-1}	0	21	52	107	214	528	1040	1428
Visual result	-	?	?	+	+	++	++	+++

Figure 2. Calibration plots for the N1 fragment. A: (Left top) RT-LAMP amplification reactions, starting from different RNA template copies (copies·µL^{-1}), (left bottom): Visual assessment of the amplification and (right) image analysis calibration curve using hue values. B: CVs recorded for end-point amplifications of different RNA copies·µL^{-1}. C: Anodic peak potential shift calibration curve. D: Intensity of current shift calibration curve at a potential of 75% the intensity at the NC peak potential. Grey dataset corresponds to the values measured but not included in the curve. Error bars represent the SD for three different amplifications. In all cases, the dashed red line corresponds to three times the SD of the non-template controls.

Sample assessment

To validate the procedure, 15 nasopharyngeal (NP) swabs of volunteering individuals taken at the HUCA were analysed. Firstly, the suitability of the medium employed for further qPCR analysis, i.e., viral transport medium (VTM), was evaluated electrochemically recording a CV under the same conditions than those for RT-LAMP-ED. This medium presented an oxidation process starting at around +0.55 mV, with current intensities up to 400 µA (data not shown), overlapping the process of PR. To overcome this, TE buffer was used as sample collection medium. Two samples were taken per individual, for RT-qPCR and RT-LAMP-ED. All samples were heat inactivated prior to analysis. This procedure has proven to be sufficient for both safety handling of SARS-CoV-2 samples [16] and extraction-free amplification [24].

Results of the here proposed method were compared with their corresponding RT-qPCR result (Figure 3). Due to the high viral load of the patients, all the positive sample electrochemical measurements were above the upper limit of the linear range and thus classified as positive. Most COVID-19 positive patients have a nasal swab viral load spanning from 10^3 to 10^{11} copies·µL^{-1} of sample [25]. Then, our low-LOD methodology, results very adequate to avoid false negative results. Apart from the thermal deactivation, the use of proteinase K for improvement of the extraction-free amplification procedure was also assessed. Results for the analysis are shown in Figure 4 (purple dataset), with this pre-treatment not showing any significant difference.

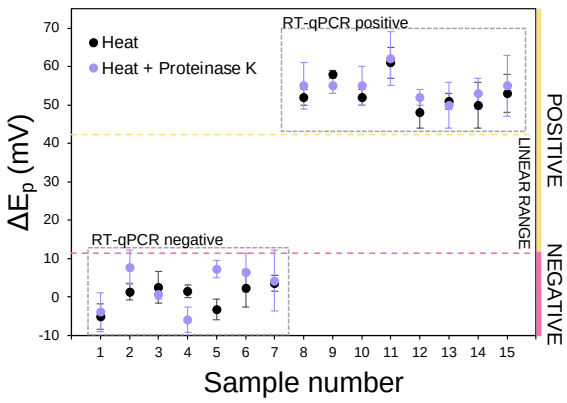

Figure 3. Clinical sample analysis. Each sample was analysed using RT-qPCR (grey boxes) and RT-LAMP-ED. For RT-LAMP-ED results, heat inactivated samples with Proteinase K (purple dataset) or without Proteinase K (black dataset) are represented in terms of shift in peak potential. Pink dashed line represents negative cut-off value, yellow dashed line represents positive non-quantifiable cut-off value. Linear range (in between) is also indicated. Error bars represent the SD for three different amplifications.

Even with a rather small sample (n=15), our RT-LAMP-ED methodology showed 100% sensitivity and specificity when compared to routine RT-qPCR performed on the corresponding laboratories. A bigger cohort study would be necessary for determining these analytical parameters with higher significance. On the other hand, although classification into positive and negative samples is the most important with special care in avoiding false negatives, quantification of highly positive samples can be of interest to monitor the infection. Therefore, a series of dilutions (1:5, 1:50 and 1:100) were prepared and assayed for quantitative purposes in three samples (Table 1).

Table 1. Clinical sample dilution analysis. For each sample, the dilution copy number was determined using the calibration curve.

Sample	Dilution	RT-LAMP-ED [RNA] (copies·µL^{-1})
10	1:5	420 ± 71
	1:50	33 ± 8
	1:100	17 ± 1
11	1:5	470 ± 30
	1:50	51 ± 9
	1:100	21 ± 1
12	1:5	350 ± 5
	1:50	33 ± 13
	1:100	12 ± 3

In all the cases, a 1:5 dilution was enough to include the analytical signal within the linear dynamic range. Therefore, quantification was possible with this dilution. Further dilutions were performed to prove the linearity of the response (Figure S6). The 1:100 dilution led to values below the linear range, and thus dilutions over this ratio should not be performed.

Towards (RT)-LAMP-ED decentralization: portable heater

To decentralize the reaction workflow, a novel heating device has been designed and implemented (Figure 4A). The main features are its small size and weight, portability, and user-friendly interface. The specifications are shown also in Figure 4A. This device has also been characterized in terms of its temperature. Figure 4B shows the values obtained for three study replicates, allowing the device to cool between studies. This portable heater showed a great performance, achieving the setpoint (65 ºC) in less than 1 min and keeping the temperature stable for at least 30 min.

For assessing the adequate performance of the RT-LAMP portable heater, amplifications were parallelly carried out under the same conditions on said heater and a commercial thermocycler. In both cases 3 negative and 3 positive (2148 copies of RNA·μL^{-1}) reactions were performed and CVs were recorded. Figure 4C shows the comparison, where the concordance in voltammetric outcomes can be seen. No significant differences in the analytical signal were observed between methods. proving the usefulness of this heater for on-site applications or for settings where a thermal cycler might not be available.

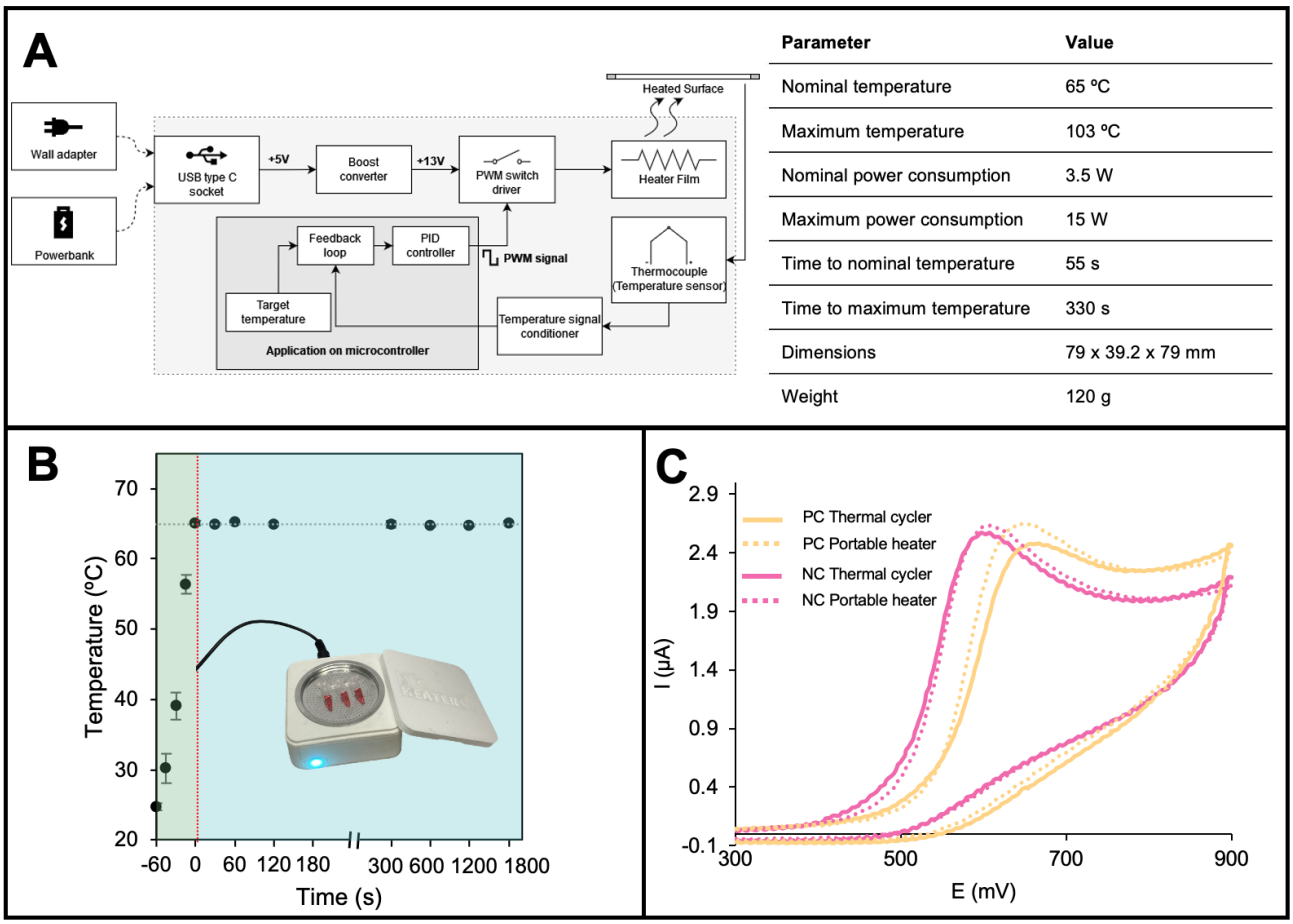

Figure 4. Portable heater for LAMP applications. A: Portable heater design, (left) circuit design, (right) heater specifications. B: Temperature assessment along the time needed for LAMP reactions. Green background indicates the device is heating, blue background indicates stable temperature. Error bars represent the SD for three different measurements. A photograph of the heater with three PCR tubes for size comparison is included as an inset. C: CVs for a batch of reactions performed on a thermal cycler and the portable heater. One CV for each batch is shown in the image. NC: Negative control; PC: Positive control.

CONCLUSIONS

In this work, we have stablished a simple, fast, and sensitive method for the electrochemical determination of SARS-CoV-2 using RT-LAMP. We have assessed three different target regions, with the N1 region showing the best performance. The analytical signal was based on changes occurring on phenol red, visual LAMP indicator already included in the master mix. During the LAMP reaction the pH changes and thus the colour and the redox process of phenol red. Five different parameters

were analysed, optical (ΔGreen and ΔHue) and electrochemical ($\Delta E_{p,}$ $\Delta I@E_{p/1.33}$ and $\Delta I@E_{p/2}$). The parameter that best fitted our purpose of decentralization was $\Delta E_{p,}$ which also presented the best linear fit. This is the first time SARS-CoV-2 is detected using this methodology. Clinical samples were analysed and compared to routine RT-qPCR results, showing 100% of sensitivity and specificity. The low LOD (theoretical: 1 copy·μL^{-1}; practical: 21 copies·μL^{-1}) makes this methodology very adequate for classification of dubious samples in a simple manner. The methodology can be easily adapted to the detection of new pathogenic threats once the sequence is known.

For decentralization purposes, a portable heater was designed, fabricated, and characterized. Its performance was evaluated against a benchtop thermal cycler, with comparable results. Work is in progress to integrate heater and potentiostat in a small device for combining amplification and detection, to advance towards pocket diagnosis.

Acknowledgements

This work was supported by the project LIFE (Fondo Supera COVID-19 from Banco Santander, CRUE and CSIC) as well as by the Spanish Government (MCIN/AEI/10.13039/501100011033) through the I+D+i projects PID2020-118376RA-I00 and PID2020-116329GB-C22. The PCTI Program of the Government of the Principality of Asturias and FEDER Program of the European Union (AYUD/2021/51289) and PCTI 2018-2022 (AYUD/2022/33539) also funded this research. This research was also supported under the project 20889/FPI/18 (Fundación Séneca, Región de Murcia, Spain). UNIR supported also the research, through the collaborative UNIR-UNIOVI project Pneumo.SARS.Detection (2021/2022). E.C.R. thanks the support of the grant “Beatriz Galindo” (BG20/00027, Ministry of Universities of the Spanish Government). Authors would like to acknowledge the technical support from Servicios Científico-Técnicos of the University of Oviedo and the Service of Microbiology and Emergency Care of the HUCA.

References

[1] M. Yüce, E. Filiztekin, K.G. Özkaya, COVID-19 diagnosis —A review of current methods, Biosens Bioelectron. 172 (2021) 112752. https://doi.org/https://doi.org/10.1016/j.bios.2020.112752.

[2] H.M. Abdelzaher, A.S. Gabr, B.M. Saleh, R.M. Abdel Gawad, A.A. Nour, A. Abdelanser, RNA Vaccines against Infectious Diseases: Vital Progress with Room for improvement., Vaccines (Basel). 9 (2021). https://doi.org/10.3390/vaccines9111211.

[3] M.G. Salomoni, Z. di Valerio, E. Gabrielli, M. Montalti, D. Tedesco, F. Guaraldi, D. Gori, Hesitant or Not Hesitant? A Systematic Review on Global COVID-19 Vaccine Acceptance in Different Populations., Vaccines (Basel). 9 (2021). https://doi.org/10.3390/vaccines9080873.

[4] P. Hardinge, J.A.H. Murray, Full Dynamic Range Quantification using Loop-mediated Amplification (LAMP) by Combining Analysis of Amplification Timing and Variance between Replicates at Low Copy Number., Sci Rep. 10 (2020) 916. https://doi.org/10.1038/s41598-020-57473-1.

[5] M. Lisboa Bastos, G. Tavaziva, S.K. Abidi, J.R. Campbell, L.P. Haraoui, J.C. Johnston, Z. Lan, S. Law, E. MacLean, A. Trajman, D. Menzies, A. Benedetti, F.A. Khan, Diagnostic accuracy of serological tests for covid-19: Systematic review and meta-analysis, The BMJ. 370 (2020). https://doi.org/10.1136/bmj.m2516.

[6] G. Turcato, A. Zaboli, N. Pfeifer, S. Sibilio, G. Tezza, A. Bonora, L. Ciccariello, D. Ausserhofer, Rapid antigen test to identify COVID-19 infected patients with and without symptoms admitted to the Emergency Department., Am J Emerg Med. 51 (2022) 92–97. https://doi.org/10.1016/j.ajem.2021.10.022.

[7] K. Uhteg, J. Jarrett, M. Richards, C. Howard, E. Morehead, M. Geahr, L. Gluck, A. Hanlon, B. Ellis, H. Kaur, P. Simner, K.C. Carroll, H.H. Mostafa, Comparing the analytical performance of three SARS-CoV-2 molecular diagnostic assays., J Clin Virol. 127 (2020) 104384. https://doi.org/10.1016/j.jcv.2020.104384.

[8] M. Inaba, Y. Higashimoto, Y. Toyama, T. Horiguchi, M. Hibino, M. Iwata, K. Imaizumi, Y. Doi, Diagnostic accuracy of LAMP versus PCR over the course of SARS-CoV-2 infection., Int J Infect Dis. 107 (2021) 195–200. https://doi.org/10.1016/j.ijid.2021.04.018.

[9] G. Xiang, X. Pu, D. Jiang, L. Liu, C. Liu, X. Liu, Development of a Real-Time Resistance Measurement for Vibrio parahaemolyticus Detection by the Lecithin-Dependent Hemolysin Gene, PLoS One. 8 (2013). https://doi.org/10.1371/journal.pone.0072342.

[10] H. Kong, W. Zhang, J. Yao, C. Li, R. Lu, Z. Guo, J. Li, C. Li, Y. Li, C. Zhang, L. Zhou, A RT-LAMP based hydrogen ion selective electrode sensing for effective detection HIV-1 RNA with high-sensitivity, Sens Actuators B Chem. 329 (2021) 129118. https://doi.org/https://doi.org/10.1016/j.snb.2020.129118.

[11] Z. Xu, K. Yin, X. Ding, Z. Li, X. Sun, B. Li, R. v. Lalla, R. Gross, C. Liu, An integrated E-Tube cap for sample preparation, isothermal amplification and label-free electrochemical detection of DNA, Biosens Bioelectron. 186 (2021). https://doi.org/10.1016/j.bios.2021.113306.

[12] D. Gosselin, M. Gougis, M. Baque, F.P. Navarro, M.N. Belgacem, D. Chaussy, A.G. Bourdat, P. Mailley, J. Berthier, Screen-Printed Polyaniline-Based Electrodes for the Real-Time Monitoring of Loop-Mediated Isothermal Amplification Reactions, Anal Chem. 89 (2017). https://doi.org/10.1021/acs.analchem.7b02394.

[13] W. Jaroenram, J. Kampeera, N. Arunrut, C. Karuwan, A. Sappat, P. Khumwan, S. Jaitrong, K. Boonnak, T. Prammananan, A. Chaiprasert, A. Tuantranont, W. Kiatpathomchai, Graphene-based electrochemical genosensor incorporated loop-mediated isothermal amplification for rapid on-site detection of Mycobacterium tuberculosis, J Pharm Biomed Anal. 186 (2020). https://doi.org/10.1016/j.jpba.2020.113333.

[14] J. Zhao, J. Gao, T. Zheng, Z. Yang, Y. Chai, S. Chen, R. Yuan, W. Xu, Highly sensitive electrochemical assay for Nosema bombycis gene DNA PTP1 via conformational switch of DNA nanostructures regulated by H+ from LAMP, Biosens Bioelectron. 106 (2018). https://doi.org/10.1016/j.bios.2018.02.003.

[15] A. González-López, M.D. Cima-Cabal, P. Rioboó-Legaspi, E. Costa-Rama, M. del M. García-Suárez, M.T. Fernández-Abedul, Electrochemical Detection for Isothermal Loop-Mediated Amplification of Pneumolysin Gene of Streptococcus pneumoniae Based on the Oxidation of Phenol Red Indicator, Anal Chem. 94 (2022) 13061–13067. https://doi.org/10.1021/acs.analchem.2c02127.

[16] C. Batéjat, Q. Grassin, J.-C. Manuguerra, I. Leclercq, Heat inactivation of the severe acute respiratory syndrome coronavirus 2., J Biosaf Biosecur. 3 (2021) 1–3. https://doi.org/10.1016/j.jobb.2020.12.001.

[17] V.L. Dao Thi, K. Herbst, K. Boerner, M. Meurer, L.P. Kremer, D. Kirrmaier, A. Freistaedter, D. Papagiannidis, C. Galmozzi, M.L. Stanifer, S. Boulant, S. Klein, P. Chlanda, D. Khalid, I. Barreto Miranda, P. Schnitzler, H.-G. Kräusslich, M. Knop, S. Anders, A colorimetric RT-LAMP assay and LAMP-sequencing for detecting SARS-CoV-2 RNA in clinical samples., Sci Transl Med. 12 (2020). https://doi.org/10.1126/scitranslmed.abc7075.

[18] W.E. Huang, B. Lim, C.-C. Hsu, D. Xiong, W. Wu, Y. Yu, H. Jia, Y. Wang, Y. Zeng, M. Ji, H. Chang, X. Zhang, H. Wang, Z. Cui, RT-LAMP for rapid diagnosis of coronavirus SARS-CoV-2., Microb Biotechnol. 13 (2020) 950–961. https://doi.org/10.1111/1751-7915.13586.

[19] C. Yan, J. Cui, L. Huang, B. Du, L. Chen, G. Xue, S. Li, W. Zhang, L. Zhao, Y. Sun, H. Yao, N. Li, H. Zhao, Y. Feng, S. Liu, Q. Zhang, D. Liu, J. Yuan, Rapid and visual detection of 2019 novel coronavirus (SARS-CoV-2) by a reverse transcription loop-mediated isothermal amplification assay, Clinical Microbiology and Infection. 26 (2020) 773–779. https://doi.org/https://doi.org/10.1016/j.cmi.2020.04.001.

[20] C.A. Schneider, W.S. Rasband, K.W. Eliceiri, NIH Image to ImageJ: 25 years of image analysis, Nat Methods. 9 (2012) 671–675. https://doi.org/10.1038/nmeth.2089.

[21] J.L. Davidson, J. Wang, M.K. Maruthamuthu, A. Dextre, A. Pascual-Garrigos, S. Mohan, S.V.S. Putikam, F.O.I. Osman, D. McChesney, J. Seville, M.S. Verma, A paper-based colorimetric molecular test for SARS-CoV-2 in saliva, Biosens Bioelectron X. 9 (2021) 100076. https://doi.org/https://doi.org/10.1016/j.biosx.2021.100076.

[22] A.T. Scott, T.R. Layne, K.C. O'Connell, N.A. Tanner, J.P. Landers, Comparative Evaluation and Quantitative Analysis of Loop-Mediated Isothermal Amplification Indicators, Anal Chem. 92 (2020) 13343–13353. https://doi.org/10.1021/acs.analchem.0c02666.

[23] M. Cerrato-Alvarez, S. Frutos-Puerto, P. Arroyo, C. Miró-Rodríguez, E. Pinilla-Gil, A portable, low-cost, smartphone assisted methodology for on-site measurement of NO2 levels in ambient air by selective chemical reactivity and digital image analysis, Sens Actuators B Chem. 338 (2021) 129867. https://doi.org/https://doi.org/10.1016/j.snb.2021.129867.

[24] D.R.E. Ranoa, R.L. Holland, F.G. Alnaji, K.J. Green, L. Wang, C.B. Brooke, M.D. Burke, T.M. Fan, P.J. Hergenrother, Saliva-Based Molecular Testing for SARS-CoV-2 that Bypasses RNA Extraction, BioRxiv. (2020). https://doi.org/10.1101/2020.06.18.159434.

[25] E.S. Savela, A. Winnett, A.E. Romano, M.K. Porter, N. Shelby, R. Akana, J. Ji, M.M. Cooper, N.W. Schlenker, J.A. Reyes, A.M. Carter, J.T. Barlow, C. Tognazzini, M. Feaster, Y.-Y. Goh, R.F. Ismagilov, Quantitative SARS-CoV-2 viral-load curves in paired saliva and nasal swabs inform appropriate respiratory sampling site and analytical test sensitivity required for earliest viral detection., MedRxiv. (2021). https://doi.org/10.1101/2021.04.02.21254771.